MIJST
MIST International Journal of Science and Technology

Numerical Modeling of Low-Velocity Impact on Composite Laminates

Diganta Chanda[1] and Md. Ashraful Islam[2*]

Department of Mechanical Engineering, Khulna University of Engineering & Technology (KUET), Khulna-9203, Bangladesh

emails: *[1]digantachanda00@gmail.com; and [*2]md.islam@me.kuet.ac.bd*

ARTICLE INFO

Article History:

Received: 17th August 2022
Revised: 27th April 2023
Accepted: 03rd May 2023
Published: 25th June 2023

Keywords:

Glass fiber reinforced polymer composite
Finite element analysis (FEA)
Hashin failure criteria
Low-velocity projectile impact

ABSTRACT

The response over the low-velocity impact of various shape impactors on a glass fiber reinforced polymer composite has been numerically analyzed with a hemispherical, flat, partially flat and truncated shaped impactor used to analyze the behavior of resistance of a GFRP composite at various speeds. The numerical analysis was carried out using finite element analysis software, ABAQUS (Dynamic/Explicit). To assess the response of the composite laminates while impacting, finite element models were developed. The Hashin failure criteria were used to represent braided glass-fiber reinforced composite plate damage. Regarding projectile shape, the impact reaction of the composite was examined. The results also show that the mechanical response of woven glass fiber polymer composite under low-velocity projectile impact largely depends on the impactor's nose shape and the velocity of the impactor.

This work is licensed under a *Creative Commons Attribution-NonCommercial 4.0 International License*.

1. INTRODUCTION

A composite material is a macroscopic blend of two or more distinct materials with a distinguishable interface. A laminate composite's distinguishing feature is its high basic strength (Sevkat *et al.*, 2009). A plastic polymer resin is used to combine thousands of tiny glass strands into fiberglass and bind them rigidly in place. Epoxy, Polyester, Vinyl ester, Polyurethane and Polypropylene are some of the most common plastic resins used in composites (Thiagarajan *et al.*, 2012). According to Sjoblom *et al.* (1988) and Shivakumar *et al.* (1985), low-speed impacts are quasi-static events involving upper limits that can vary from one ms^{-1} to ten ms^{-1} depending on the mass and stiffness of the impactor, the stiffness of the target, and perhaps other criteria. The low-velocity effect, the structurally dynamic reaction of the target, is crucial because the contact time allows the entire system to react to the hit, increasing the amount of energy elastically absorbed. (Sjoblom *et al.*, 1988) (Shivakumar *et al.*, 1985). The laminate's impact resistance is determined by various parameters, including inter-laminar strengths, stacking sequence, impacting item size, velocity and mass of the impactor. Whenever a structure comprised of composite material is in interaction with a foreign object, fiber breakage, delamination, matrix cracking, and plastic deformations due to contact are only a few effects to consider(Richardson & Wisheart, 1996). Materials in the matrix phase are usually continuous. A foreign body has an influence on the composite material (Singh & Shinde, 2022). Liu and Malvern (1987) proposed that the type of impact can be classified based on the amount of damage sustained, particularly if damage is the primary concern. Penetration-induced fiber breakage characterizes high velocity, while delamination and matrix cracking characterize low velocity (Liu & Malvern, 1987). Robinson and Davies (1992) used laboratory coupon testing results to examine the damage tolerance of brittle composite structures, analyzing the effect of impactor weight and specimen design size on the low-velocity impact performance of a variety of woven fiber reinforced composite laminates. Safri *et al.* (2014) illustrated the deformation and damage mechanisms involved throughout the impact of objects in formulating appropriate composite structures to improve the survivability of aircraft structures regarding low and high-velocity impacts. For epoxy composites, this results in the transition to the impact of energy can be measured if height and weight are known. Though appropriate techniques for detection can be used for quantification. The seriousness of such losses could be low-speed impacts considered to be dangerous loads because they influence the efficiency of the composite (Cawley, 1989) (Amaro *et al.*, 2012). Kurşun *et al.* (2016) was using an experimental procedure and ABAQUS validation to investigate the impact issue, establishing that impactor shape has a major impact on damage pattern and stress distribution. They also discovered that with a low-

velocity impact, a flat cylindrical impactor generates the maximum damage to the laminate, whereas a smaller contact area causes less damage (Kurşun *et al.*, 2016). Finite element measurements have been extrapolated to composites of multiple shapes, compositions, sizes, forces, and boundary conditions, without incurring the cost and time associated with physical processing. Once validated with experimental evidence, FE models may yield incredibly valuable findings in a wide range of scenarios (Moura & Marques, 2002) (Sridhar & Rao, 1995). Hosur *et al.* (2005) performed a test for low-speed impacts with a hemispherical impactor on thin hybrid composites. They found that the carriage performance of hybrid composites was increased considerably in contrast to carbon/epoxy strains with a marginal decrease in rigidity (Hosur *et al.*, 2005). Another study presented the energy of impact, the diameter of the impactor and sandwich boards, such as the core thickness of the foam and thickness of the face boards on impact behavior and impact damages (Wang *et al.*, 2013). The impact response of two hybrid composites with comparable glass and graphite fabric compositions but different lay-up arrangements were investigated by Sevkat *et al.* (2013). The results indicate a higher force, greater delamination among hybrid layers and short contact duration for impactors with a larger contact surface (Sevkat *et al.*, 2013). Zhou (1995) has had a low-speed effect with a flat-ended impactor on glass-enhanced laminates made of tissue. The structural features of these structures for impact damage are influenced by geometry (Zhou, 1995). Mitrevski *et al.* (2006) investigated the impact of impactor form on the effects of thin tissue laminates carbon-epoxy experimentally. The various impactor forms have greatly impacted mechanisms for damage (Mitrevski *et al.*, 2006). A research study investigated the impact response of woven glass–epoxy laminates, and their findings illustrate the impact and Compression After Impact (CAI) influence of the projectile diameter (Icten *et al.*, 2013). The glass/epoxy-laminated composite plate's low-velocity impact loading behavior was examined in relation to the effect of biaxial preloading experimentally and numerically (Kurşun *et al.*, 2015). Drop weight impact is used in experimental tests for low-velocity effect, and the weights may be of various shapes, as well as a pendulum type test. Another research study investigated the LVI phenomenon on hybrid composite beams using the Charpy effect method (Rawat *et al.*, 2017). Sevkat *et al.* (2013) investigated the effects of drop weight on hybrid composites. The analysis was focused on experimentation and was validated using LS-DYNA (Sevkat *et al.*, 2013). Shashikumar (2015) investigated the performance of glass fiber reinforced polymer composite laminates under the low-velocity influence using the explicit finite element analysis tool LS-DYNA. The numerical and analytical conclusions were compared to existing experimental data from the literature study regarding overall impact force and energy. The variation in empirical, laboratory and analytical values was less than 10%, suggesting that the results were within a reasonable estimation range (Shashikumar, 2015). Bouvet *et al.* (2012) used a numerical model to capture the various types of damage that can occur in composite laminates when they are subjected to a low-velocity/low energy impact. Three types of damage were considered in their numerical model: fiber failure, matrix cracking and delamination (Bouvet *et al.*, 2012). There is a scarcity of studies that examined the influence of impactor shapes on the impact response of composite sandwich plates, necessitating the collection of more data on the response of sandwich structures to low-velocity impact. Therefore, a numerical investigation on the glass fiber reinforced polymer composite to analyze the behavior of resistance of a GFRP composite at various speeds of energy impact.

Modeling the composite as an orthotropic elastic material allowed for the preliminary elastic response of the woven glass fiber laminate to be identified. The values of elastic modulus E_1, E_2, E_3, Poisson's ratios ϑ_{12}, ϑ_{13}, ϑ_{23} and shear modulus G_{12}, G_{13}, and G_{23} are utilized to describe the composite. The density of the glass fiber was calculated to be 1,800 kg/m^3. The mass of all impactors is 1.5kg and is assigned to the reference point of the impactor.

2. MATERIALS AND SYSTEM MODELING

The composite investigated in this simulation comprised of four plies of GFRP composite laminates, where each ply was 0.1 mm thick. The fiber orientation of this composite is 0/90/90/0. The dimension of the GFRP composite laminate is 72mm x 72 mm.

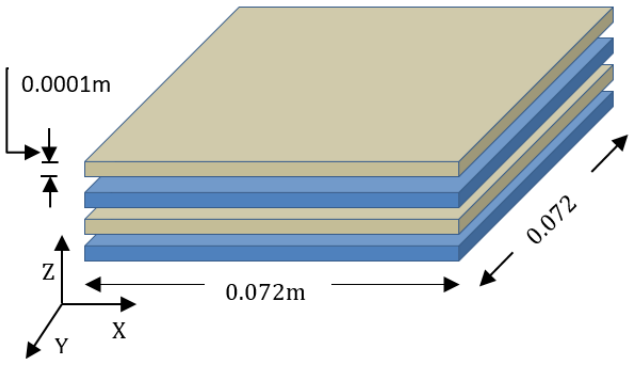

Figure 1: Dimension of GFRP composite plate

The numerical model was analyzed using four distinct types of impactors. All of these impactors' dimensions are specified in millimeters, and the complete length of these impactors from top to bottom surface is 30 mm. Epoxy polymer matrix is used in this glass fiber polymer composite. Uniform requirements might be used with an element removal technique for damage initiation to remove Abaqus rejected elements. Below are the values for X^T, X^C, Y^T, Y^C, S^L, and S^T.

Table 1
Properties of the glass fiber laminates utilized in this study (Fan *et al.*, 2011)

E_1 (GPa)	E_2 (GPa)	E_3 (GPa)	V_{12}	V_{13}	V_{23}	G_{12} (GPa)	G_{13} (GPa)	G_{23} (GPa)
25	23	5	.15	.15	.15	5	5	5

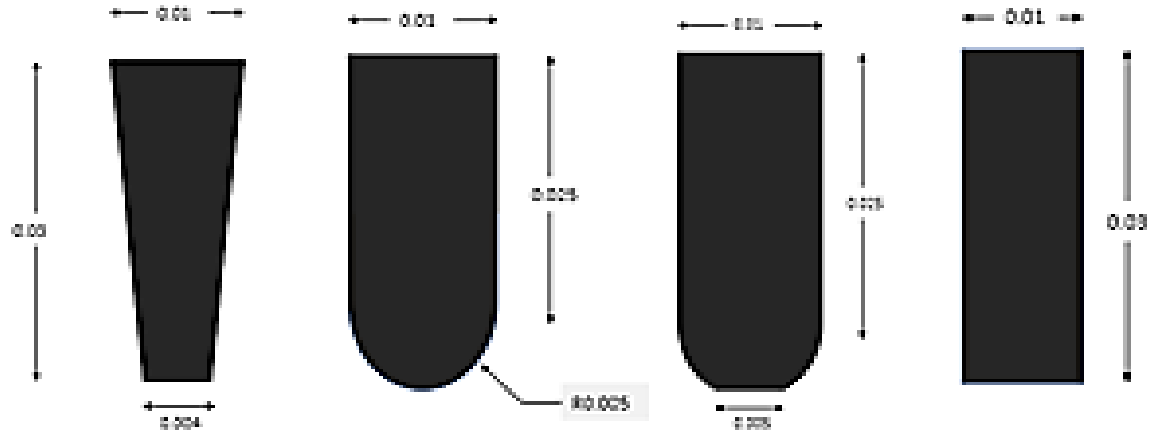

Figure 2: (a) Truncated Impactor (b) Hemispherical Impactor (c) Partially flat Impactor (d) Flat Impactor

Table 2
Damage initiation data of the glass fiber laminates utilized in this study (Fan *et al.,* 2011)

X^T (MPa)	X^C (MPa)	Y^T (MPa)	Y^C (MPa)	S^L (MPa)	S^T (MPa)
320	240	320	240	320	320

X_T, and X_C represent tensile and compressive strengths in the longitudinal direction. Y_T and Y_C represent tensile and compressive strengths in the transverse direction. S_L and S_T represent longitudinal and transverse shear strengths.

After damage initiation, the negative slope of equivalent load-displacement relation is used to simulate damage progression. The value required for damage progression is given below

Table 3
Fracture energies for damage progression of composite laminate(Fan *et al.,* 2011)

Longitudinal tensile fracture Energy (J/m²)	Transverse tensile fracture Energy (J/m²)	Longitudinal compressive fracture Energy (J/m²)	Transverse compressive fracture Energy (J/m²)
40000	40000	60000	60000

This investigation defined contact and interaction using a general contact method and a contact pair algorithm. Both methods use advanced tracking algorithms to ensure that adequate contact conditions are properly maintained and they may be employed concurrently in a model. To simulate the interaction between GFRP plates subjected to projectile impact, a surface-to-surface contact pair was created. between the projectile surface and the nodes-set at the target center of each layer. In contrast, a general contact interaction was constructed between the two adjacent layers. The contact interaction characteristics applied in this study are presented in Table 4.

A. Modeling Progressive Damage

There are four main modes of failure (though several others may be referred to) since fiber-reinforced plastic (FRP) laminates are heterogeneous and anisotropic: mode-cracking matrix happens in parallel with fibers because of stress, compression or shear, mode-derived, delamination of inter-laminar strain, fiber splitting and un-compressed fiber buckling mode-in-tension fiber, the impactor perforates the impacted area completely. Identify the fault mode since this would provide information not only on the impact event but also on the residual intensity of the structure. In understanding damage mode starts and develops, interactions between failure modes are also significant. Applying Hashin's failure criterion, the composite's damage initiation was designed. These criteria use a total of four different types of damage-initiation mechanisms: matrix tension, matrix compression, fiber tension, and fiber compression. The initial failure criteria are as follows:

Fiber tension:

$$F_f^t = \left(\frac{\tilde{\sigma}_{11}}{X^T}\right)^2 + \alpha\left(\frac{\tilde{\tau}_{12}}{S^L}\right)^2, \tilde{\sigma}_{11} \geq 0 \quad (1)$$

Fiber compression:

$$F_f^c = \left(\frac{\tilde{\sigma}_{11}}{X^C}\right)^2, \tilde{\sigma}_{11} < 0 \quad (2)$$

Matrix tension:

$$F_m^t = \left(\frac{\tilde{\sigma}_{11}}{Y^T}\right)^2 + \left(\frac{\tilde{\tau}_{12}}{S^L}\right)^2, \tilde{\sigma}_{22} \geq 0 \quad (3)$$

Matrix compression:

$$F_m^c = \left(\frac{\tilde{\sigma}_{22}}{2S^T}\right)^2 + \left[\left(\frac{Y^C}{2S^T}\right)^2 - 1\right]\frac{\tilde{\sigma}_{22}}{Y^C} + \left(\frac{\tilde{\tau}_{12}}{S^L}\right)^2, \tilde{\sigma}_{22} < 0 \quad (4)$$

The damage elastic matrix can be represented as,

$$C_d = \frac{1}{D}\begin{bmatrix} (1-d_f)E_1 & (1-d_f)(1-d_m)v_{21}E_1 & 0 \\ (1-d_f)(1-d_m)v_{12}E_2 & (1-d_m)E_2 & 0 \\ 0 & 0 & (1-d_s)GD \end{bmatrix} \quad (5)$$

$\tilde{\sigma}_{11}$ is the longitudinal effective stress tensor component, $\tilde{\sigma}_{22}$ is transverse effective stress tensor component and $\tilde{\tau}_{12}$ is shear effective stress tensor component and α represents the contribution of shear stress to the fiber tensile initiation criterion. G is the shear modulus, while D is the total damage variable, linking stress and strain to demonstrate stress deterioration. In the equation above, d_f stands for the current state of fiber damage, d_m for the current state of matrix damage, d_s for the current state of shear damage, and C_d for the current state of the damaged elastic matrix.

Table 4
Contact interaction properties used in this study (Fan *et al.*, 2011)

Interaction	Contact Algorithms	Friction Formulations	Friction-coefficient	Pressure Overclosure	Contact-stiffness
Impactor-GFRP	Contact pair	Penalty	0.6	Hard	Hard
GFRP-GFRP	General-contact	Penalty	0.3	linear	15 GPa

Through numerical modeling using the ABAQUS software, the stress distribution on the GFRP laminate as a result of the low-velocity impact will be determined (Dynamic, Explicit). Development and use of sophisticated numerical techniques based on the Finite Element Method are among the project's endeavors (FEM). The effect of material constants on the stress singularity will be examined using the developed numerical model. Geometry modeling was done initially. There was a 0.1 mm distance between the impactor tip and composite plate top surface, so there may not occur any initial damage. Then the plate's characteristics were unveiled. Following the creation of the step, the model's boundary conditions were applied. The side face of the composite plate is fixed (U1=U2=U3=0). The impactor's only allowed direction of movement is in the Z direction. Neither axis is rotated, as well as no X or Y movement. The weight is assigned at the impactor's reference point. Different speeds are supplied as a pre-defined value for the loading situation. Meshwork was the last phase. The element shape for composite laminate is Hex, and the technique was structured. Reduced integration with hourglass control, an 8-node quadrilateral

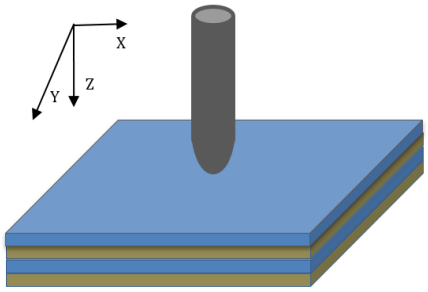

Figure 3: Geometrical modeling of low-velocity impact on GFRP composite laminate

in-plane general-purpose continuum shell, and finite membrane stresses make up the SC8R element type used in the meshing. The element shape for all four impactors is Quad-dominated, and the technique was a sweep. The element type of the meshing is R3D4: A 4-node 3-D bilinear rigid quadrilateral.

3. RESULT AND DISCUSSION

A. Mesh Sensitivity Analysis

The element size is maximum on the edge of the composite laminates and minimum in the center of the composite laminates. The maximum size is 1 mm, and the minimum size is 0.75 mm. As element size decreases, the peak load of this model also can be observed. Peak load values for element sizes of 0.5mm, 0.25 mm, and 0.1 mm are nearly constant having started at 0.75mm element size.

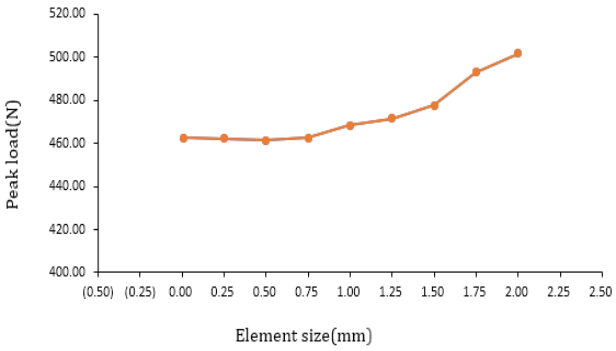

Figure 4: Mesh Independency test

B. Model Validation

The numerical data was validated with experimental data and the final model was developed. The graph plotted in Figure 5 shows the FE and experimental curve of impact load on the composite plate against time. For both conditions, the peak load was almost similar. But, there is a little discrepancy between the numerical result and the experimental results in the case of time. This happened due to not assigning the velocity-time amplitude. The velocity-time data was not given the pre-determined velocity used in the loading condition. Because of this numerical model graph was slightly different from the research paper load against the time graph.

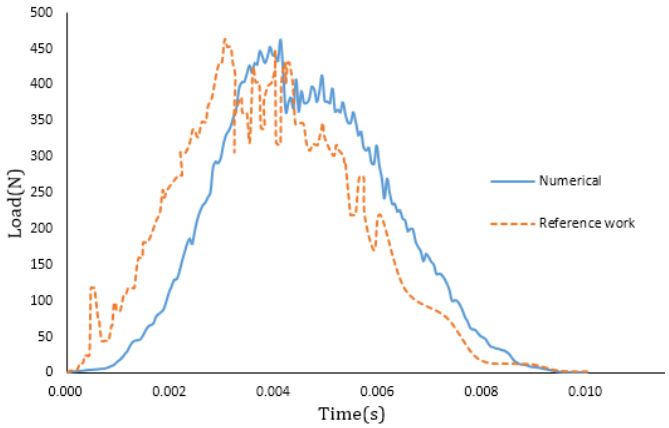

Figure 5: Simulation result and experimental (Fan *et al.*, 2011) work comparison based on load against time

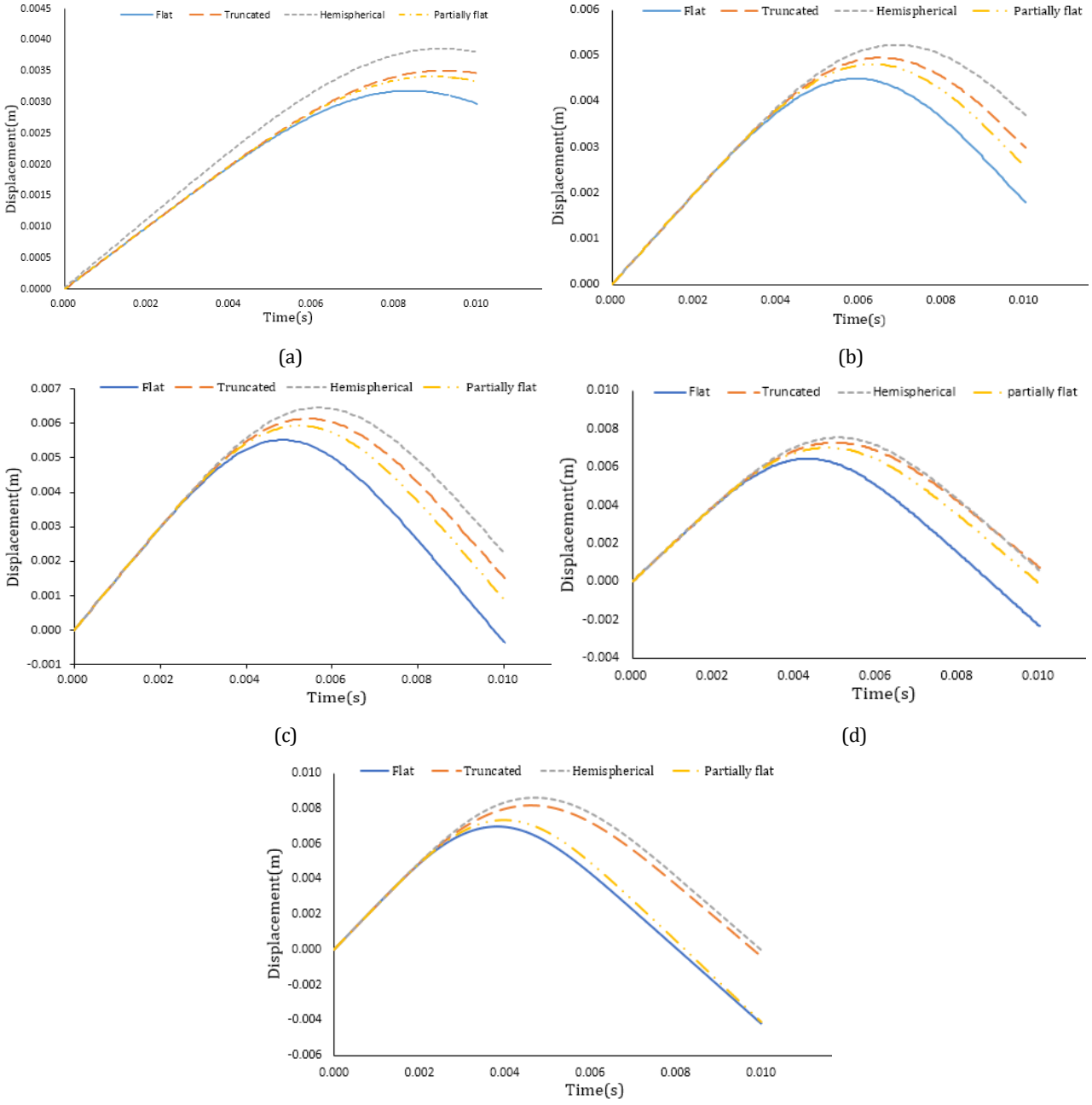

Figure 6: Load v/s Time at (a) 0.5 ms^{-1} (b) 1 ms^{-1} (c) 1.5 ms^{-1} (d) 2 ms^{-1} (e) 2.5 ms^{-1} velocity

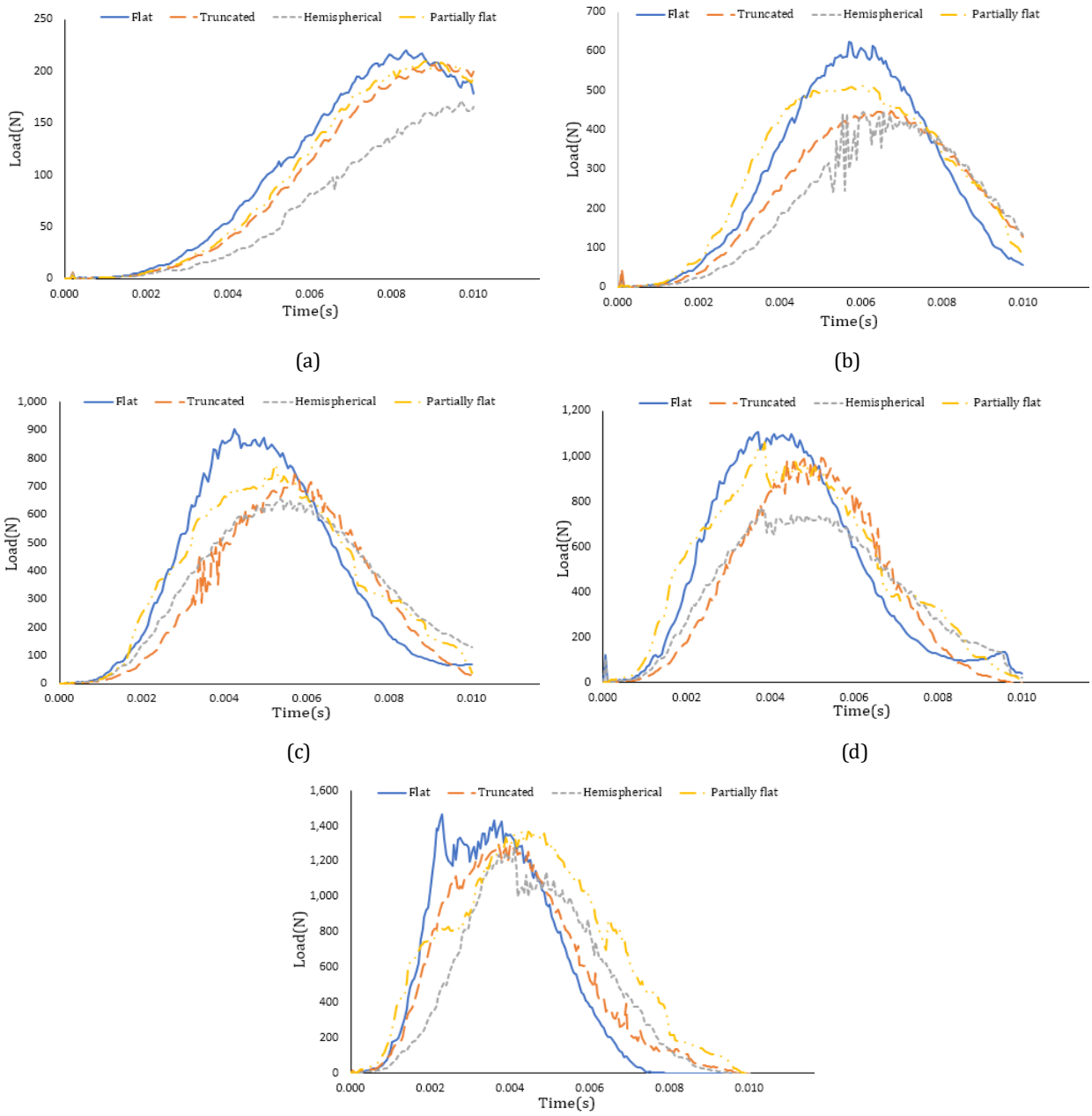

Figure 7: Displacement v/s Time at (a) 0.5 ms^{-1} (b) 1 ms^{-1} (c) 1.5 ms^{-1} (d) 2 ms^{-1} (e) 2.5 ms^{-1} velocity

The load-time curves of four distinct types of impactor's low-velocity impact on the composite plate at different velocities are illustrated in Figure 6. The load-time curves have parabolic shapes, and the maximal contact force is greatest when the impact energy is low and increases as the impact energy does. The response force applied from the specimen to the impactor is sometimes called the contact force. As was already noted, all information was gathered using the ABAQUS program to determine how the contact force varied with contact time. Due to its enormous surface area, the flat impactor produces the maximum peak load. The peak load of a partially flat impactor is hence lower than the flat impactor because the tip surface area is less than the flat impactor. Since it has a smaller surface area, the truncated impactor's peak load is less than that of the partially flat and flat-shaped impactor. Since the hemispherical impactor's tip surface area is the lowest, it produces the lowest peak load among the four impactors. As seen in Figure 6 sequentially, it is clear that the peak load increases with increasing velocity and the graph pattern changes slightly. Stress was produced throughout the perimeter owing to shear force for impactors with flat, partially flat, and truncated shapes that struck the top surface of composite plates. In contrast, the center of a hemispherical-shaped impactor produces stress when it makes contact with the plate top surface.

All four plies of the composite plate experienced internal stress as a result of the collision and comparatively at a greater velocity, di-lamination in the composite plate was initiated.

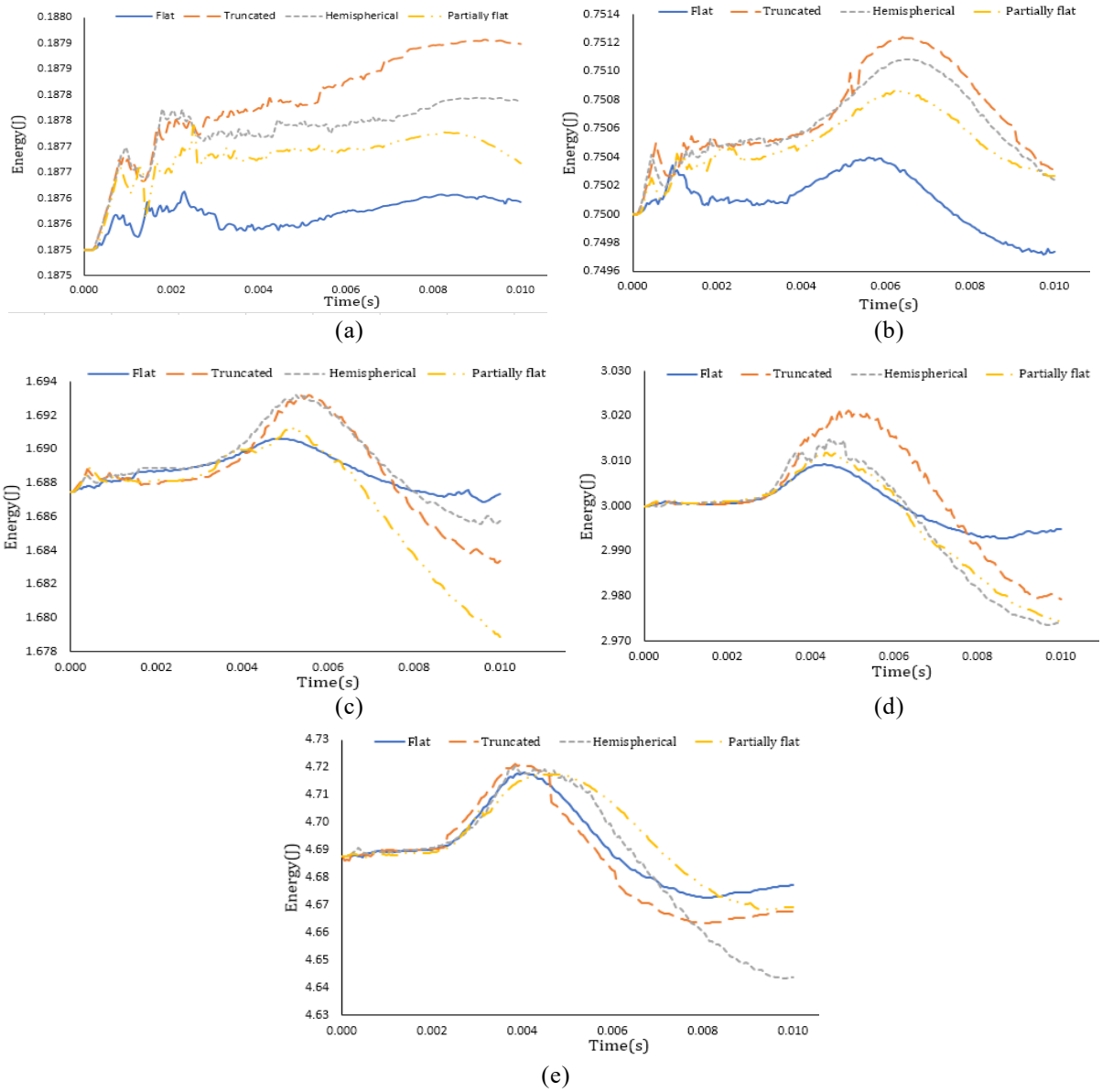

Figure 8: Energy v/s Time at (a) 0.5 ms^{-1} (b) 1 ms^{-1} (C) 1.5 ms^{-1} (d) 2 ms^{-1} and (e) 2.5 ms^{-1} velocity

Figure 7 depicts displacement versus time curves for four distinct shaped impactors at 0.5 ms^{-1}, 1 ms^{-1}, 1.5 ms^{-1}, 2 ms^{-1}, and 2.5 ms^{-1}, respectively. Hemispherical impactor has the maximum displacement: As it has the least tip area, stress is concentrated and displacement is high. A little less displacement is produced by the impactor truncated, and the somewhat flat impactor produces even less. The impactor with a flat form has the least displacement because the tip surface area of the flat impactor is the biggest among them. With increasing time, displacement increases gradually, but after maximum, displacement decreases with increasing time as the impactor returns to the initial position and some impactor ray beyond the initial position at comparatively higher velocity.

Figure 8 shows the total energy of the whole model against the time graph plotted for four distinct shaped impactors at 0.5 ms^{-1}, 1 ms^{-1}, 1.5 ms^{-1}, 2 ms^{-1}, and 2.5 ms^{-1}, respectively. As seen in Figure 8 impactor hit the composite plate with the initial kinetic energy of 0.1875J, 0.75J, 1.6875 J, 3J, and 4.6875J sequentially. During an impact event, the energy absorbed by the laminates is dissipated through the damage formation. Initially, energy increases over time because of increasing strain energy of the plate, but after attaining maximum energy, the energy declines over time due to creep, friction and damage absorption. Among all impactors, energy variation tends to be identical at relatively high velocities.

4. CONCLUSIONS

The low-velocity effect on the GFRP composite has been quantitatively modeled in this experiment using the finite element analysis software ABAQUS. This model was developed to compare the variation of energy for the entire model and study the stress field of the composite plate at different velocities for various shape impactors. Since a flat-shaped impactor has the maximum contact time with the least amount of displacement, it also carries the most stress on the contact surface. The hemispherical shape impactor has the least amount of contact time with the greatest amount of displacement, generating the least amount of stress on the contact

surface. In this research, five different pre-determined velocities were assigned to all impactors, and it was seen that with increasing velocity load in the contact surface and displacement increase. Also, with increasing velocity, the energy variation with respect to time tends to be indistinguishable for all four impactors. For truncated, partially flat and flat impactors stress is generated where the impactor's perimeter hits the plate, and for hemispherical impactors, stress is generated in the center of the composite plate where impacted. The inter-laminar stress field was also analyzed, and it was seen that de-lamination between plies occurred with increasing velocity.

ACKNOWLEDGEMENTS

The authors woulld like to express their gratitude to the Department of Mechanical Engineering, Khulna University of Engineering and Technology, Khulna, Bangladesh. We also would lilke to thank Palash Das and Samiul Alam for assisting in learning the ABAQUS software.

REFERENCES

Amaro, A. M., Reis, P. N. B., de Moura, M. F. S. F., & Santos, J. B. (2012). Damage detection on laminated composite materials using several NDT techniques. *Insight - Non-Destructive Testing and Condition Monitoring*, *54*(1), 14–20. https://doi.org/10.1784/insi.2012.54.1.14

Bouvet, C., Rivallant, S., & Barrau, J. J. (2012). Low velocity impact modeling in composite laminates capturing permanent indentation. *Composites Science and Technology*, *72*(16), 1977–1988. https://doi.org/10.1016/j.compscitech.2012.08.019

Cawley, P. and R. A. (1989). *Defect types and non-destructive testing techniques for composites and bonded joints. Materials science and technology, 1989. 5(5): p. 413-425.* *5*(May), 413–425.

de Moura, M. F. S. F., & Marques, A. T. (2002). Prediction of low velocity impact damage in carbon–epoxy laminates. *Composites Part A: Applied Science and Manufacturing*, *33*(3), 361–368. https://doi.org/10.1016/S1359-835X(01)00119-1

Fan, J., Guan, Z., & Cantwell, W. J. (2011). Modeling perforation in glass fiber reinforced composites subjected to low velocity impact loading. *Polymer Composites*, *32*(9), 1380–1388. https://doi.org/10.1002/pc.21161

Hosur, M. V., Adbullah, M., & Jeelani, S. (2005). Studies on the low-velocity impact response of woven hybrid composites. *Composite Structures*, *67*(3), 253–262. https://doi.org/10.1016/j.compstruct.2004.07.024

Icten, B. M., Kıral, B. G., & Deniz, M. E. (2013). Impactor diameter effect on low velocity impact response of woven glass epoxy composite plates. *Composites Part B: Engineering*, *50*, 325–332. https://doi.org/10.1016/j.compositesb.2013.02.024

Kurşun, A., Şenel, M., & Enginsoy, H. M. (2015). Experimental and numerical analysis of low velocity impact on a preloaded composite plate. *Advances in Engineering Software*, *90*, 41–52. https://doi.org/10.1016/j.advengsoft.2015.06.010

Kurşun, A., Şenel, M., Enginsoy, H. M., & Bayraktar, E. (2016). Effect of impactor shapes on the low velocity impact damage of sandwich composite plate: Experimental study and modelling. *Composites Part B: Engineering*, *86*, 143–151. https://doi.org/10.1016/j.compositesb.2015.09.032

Liu, D., & Malvern, L. E. (1987). Matrix Cracking in Impacted Glass/Epoxy Plates. *Journal of Composite Materials*, *21*(7), 594–609. https://doi.org/10.1177/002199838702100701

Mitrevski, T., Marshall, I. H., Thomson, R. S., & Jones, R. (2006). Low-velocity impacts on preloaded GFRP specimens with various impactor shapes. *Composite Structures*, *76*(3), 209–217. https://doi.org/10.1016/j.compstruct.2006.06.033

Rawat, P., Singh, K. K., & Singh, N. K. (2017). Numerical investigation of damage area due to different shape of impactors at low velocity impact of GFRP laminate. *Materials Today: Proceedings*, *4*(8), 8731–8738. https://doi.org/10.1016/j.matpr.2017.07.222

Richardson, M. O. W., & Wisheart, M. J. (1996). Review of low-velocity impact properties of composite materials. *Composites Part A: Applied Science and Manufacturing*, *27*(12), 1123–1131. https://doi.org/10.1016/1359-835X(96)00074-7

Robinson, P., & Davies, G. A. O. (1992). Impactor mass and specimen geometry effects in low velocity impact of laminated composites. *International Journal of Impact Engineering*, *12*(2), 189–207. https://doi.org/10.1016/0734-743X(92)90408-L

Safri, S. N. A., Sultan, M. T. H., Yidris, N., & Mustapha, F. (2014). Low velocity and high velocity impact test on composite materials – A review. *The International Journal of Engineering and Science (IJES)*, *3*(9), 50–60. https://doi.org/10.1177/1464420711409985

Sevkat, E., Liaw, B., & Delale, F. (2013). Drop-weight impact response of hybrid composites impacted by impactor of various geometries. *Materials & Design (1980-2015)*, *52*, 67–77. https://doi.org/10.1016/j.matdes.2013.05.016

Sevkat, E., Liaw, B., Delale, F., & Raju, B. B. (2009). Drop-weight impact of plain-woven hybrid glass–graphite/toughened epoxy composites. *Composites Part A: Applied Science and Manufacturing*, *40*(8), 1090–1110. https://doi.org/10.1016/j.compositesa.2009.04.028

Shashikumar R, *et al.* (2015). *Finite element analysis of Low Velocity Impact on Woven Type Gfrp Composite*. *3*(1), 105–110.

Shivakumar, K. N., Elber, W., & Illg, W. (1985). Prediction of low-velocity impact damage in thin circular laminates. *AIAA Journal*, *23*(3), 442–449. https://doi.org/10.2514/3.8933

Singh, K. K., & Shinde, M. (2022). *Low Velocity Impact on Fibre Reinforced Polymer Composite Laminates* (pp. 83–105). https://doi.org/10.1007/978-981-16-9439-4_3

Sjoblom, P. O., Hartness, J. T., & Cordell, T. M. (1988). On Low-Velocity Impact Testing of Composite Materials. *Journal of Composite Materials*, *22*(1), 30–52. https://doi.org/10.1177/002199838802200103

Sridhar, C., & Rao, K. P. (1995). Estimation of low-velocity impact damage in laminated composite circular plates using nonlinear finite element analysis. *Computers & Structures*, *54*(6), 1183–1189. https://doi.org/10.1016/0045-7949(94)00404-Q

Thiagarajan, A., Palaniradja, K., & Alagumurthi, N. (2012). Low velocity impact analysis of nanocomposite laminates. *International Journal of Nanoscience*, *11*(3), 115–125. https://doi.org/10.1142/S0219581X1240008X

Wang, J., Waas, A. M., & Wang, H. (2013). Experimental and numerical study on the low-velocity impact behavior of foam-core sandwich panels. *Composite Structures*, *96*, 298–311. https://doi.org/10.1016/j.compstruct.2012.09.002

Zhou, G. (1995). Damage mechanisms in composite laminates impacted by a flat-ended impactor. *Composites Science and Technology*, *54*(3), 267–273. https://doi.org/10.1016/0266-3538(95)80019-0